Food Chemistry: X 22 (2024) 101407

Contents lists available at ScienceDirect

Food Chemistry: X

journal homepage: www.sciencedirect.com/journal/food-chemistry-x

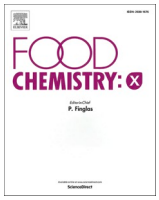

The role of water distribution, cell wall polysaccharides, and microstructure on radish (*Raphanus sativus* L.) textural properties during dry-salting process

Qianqian Jiang [a,b], Shuang Zhao [b], Wenting Zhao [b], Pan Wang [b], Peiyou Qin [b], Junjuan Wang [b], Yuanyuan Zhao [b], Zhiwen Ge [b], Xiaoyan Zhao [a,b,*], Dan Wang [a,b,*]

[a] *College of Food Science, Shenyang Agricultural University, Shenyang, Liaoning 110866, China*
[b] *Institute of Agri-food Processing and Nutrition, Beijing Academy of Agriculture and Forestry Sciences, Beijing Key Laboratory of Fruits and Vegetables Preservation and Processing, Key Laboratory of Vegetable Postharvest Processing, Ministry of Agriculture and Rural Affairs, Beijing 100097, China*

ARTICLE INFO

Keywords:
Radish (*Raphanus sativus* L.)
Salting process
Texture
Water distribution
Pectin content
Microstructure

ABSTRACT

Radish (*Raphanus sativus* L.) undergoes texture changes in their phy-chemical properties during the long-term dry-salting process. In our study, we found that during the 60-day salting period, the hardness and crispness of radish decreased significantly. In further investigation, we observed that the collaborative action of pectin methylesterase (PME) and polygalacturonase (PG) significantly decreased the total pectin, alkali-soluble pectin (ASP), and chelator-soluble pectin (CSP) content, while increasing the water-soluble pectin (WSP) content. Furthermore, the elevated activities of cellulase and hemicellulase directly led to the notable fragmentation of cellulose and hemicellulose. The above reactions jointly induced the depolymerization and degradation of cell wall polysaccharides, resulting in an enlargement of intercellular spaces and shrinkage of the cell wall, which ultimately led to a reduction in the hardness and crispness of the salted radish. This study provided key insights and guidance for better maintaining textural properties during the dry-salting process of radish.

1. Introduction

Salted vegetables, a traditional Chinese fermented food product highly favored by consumers, are widely used as side dishes or appetizers (Wei et al., 2022). It is mainly made of vegetables as the main raw material, processed through techniques such as immersion in edible salt or saline solution, with the optional addition of supplementary ingredients. Based on the aforementioned classification criterion, the processing methods of salted vegetables can be categorized into dry-salting, wet salting (soaking in edible salt water), and mixed salting (salt water plus ginger, red pepper, garlic, onion, and vinegar et al.) (Liu et al., 2017). Dry-salting, the simplest, typical, and widely produced salted vegetable processing method by small-scale factories or households, can make the salting liquid more concentrated, thereby enhancing the flavor of the vegetables. In addition, dry-salting at low temperatures increases the safety and extends the shelf life of vegetables by delaying the growth of microorganisms.

Texture stands as a crucial quality indicator in assessing the market value and consumer acceptance of salted vegetables. In recent years, researchers in salted vegetable production field have increasingly recognized that the texture changes during the salting process varied greatly among different vegetable types. For instance, Yang et al. (2023) observed twice "increase–decrease" texture changes of kohlrabi during the complex pickling procedures, while Ye et al. (2022) found that the hardness and crispness of chili peppers decreased gradually with prolonged salting time. Studying the underlying regularities of these complex textural changes can provide crucial guidance for the processing of salted vegetables. In previous studies, the mechanism of vegetable texture changes was thought to be primarily associated with alterations in cell wall polysaccharides, water status, and cellular structure induced by the processing (Li et al., 2018; Lu et al., 2021).

White radish (*Raphanus sativus* L.), belonging to the Brassicaceae family, is a vegetable widely cultivated and consumed around the world. It is rich in various nutritional components (e.g., flavonoids, sulforaphane, dietary fiber, β-carotene, and minerals), exhibiting potent antioxidant and anti-cancer effects (Gamba et al., 2021). Thus, radish is always employed in the production of salted processed products with good flavor and taste properties. However, the texture changes of radish

* Corresponding authors at: College of Food Science, Shenyang Agricultural University, Shenyang, Liaoning 110866, China.
E-mail address: wangdan@iapn.org.cn (D. Wang).

https://doi.org/10.1016/j.fochx.2024.101407
Received 17 February 2024; Received in revised form 8 April 2024; Accepted 21 April 2024
Available online 23 April 2024

during long-term dry-salting at low temperature (4 °C) have not been reported yet. Additionally, the role of water distribution, cell wall polysaccharides, and microstructure on radish textural properties of the typical dry-salting method under low-salt conditions during the salting process remains unclear.

Therefore, this work aimed to (i) reveal the rule of texture changes in dry-salted radish during long-term dry-salting; (ii) clarify the impact of comprehensive changes in water distribution, cell wall polysaccharides, and cell microstructure on the textural properties of salted radish; (iii) summarize the texture evolution mechanism of dry-salting radish and provide effective process guidance for their industrial production according to the experimental outcomes.

2. Materials and methods

2.1. Chemicals

All kits (KIRbio) for this experiment were provided by Beijing JINZHIYAN Biotechnology Co., Ltd. (Beijing, China). The required chemical reagents (i.e., concentrated sulfuric acid, acetone, ethanol, and glutaraldehyde) were all of analytical grade (greater than or equal to 95% purity) and supplied by Bailingwei Technology Co., Ltd. (Beijing, China).

2.2. Sample preparation

Fresh white radish samples ("White-Jade Chun" variety) were purchased from a local market in Beijing, China. The samples were washed with water to remove surface contaminants and the surface moisture was wiped with sterile gauze. Subsequently, the head and tail tissues from the radish were removed and the remaining tissues were cut into strips (approximately 7 cm × 1 cm × 1 cm) using a clean knife. Afterwards, the fresh edible radish strips (marked as Fresh) were subjected to natural air drying for 24 h (temperature ranging from 10 to 22 °C, with approximately 45% humidity), facilitating dehydration to approximately 50% of their fresh weight. Finally, dehydrated radishes with salt in a ratio of 5% to the weight of the radish were kneaded till the salt was fully dissolved, thereafter, salted radish samples (500 g) were put into a sterile glass jar for sealing. Eventually, the sealed samples were stored at 4 °C for 60 days, sampling was conducted at 0, 15, 30, 45, and 60 days for texture analysis, water distribution assessment, cell wall polysaccharide component content determination, pectin-related enzyme detection, and scanning electron microscopy observations. Three parallel samples were taken at each time point. The results were marked as Fresh, D0, D15, D30, D45, and D60, respectively.

2.3. Texture analysis

Textural properties of hardness (N) and brittleness (mm) were determined using a texture analyzer with a P/5 N probe (TAXT-Plus, Stable Micro Systems, Surrey, UK). The test parameters were as follows: test mode, compression; test speed, 0.5 mm/s; post-test speed, 15 mm/s; target mode, distance; distance, 9 mm; trigger type, button; advanced options, Off. Notably, the radish strips with uniform thickness were selected before a test and each sample was tested 18 times.

2.4. Water distribution

2.4.1. Low-field nuclear magnetic resonance (LF-NMR)

A low-field nuclear magnetic resonance (LF-NMR) analyzer (NMI20-025 V-I, New Mai Electric Co., Ltd., Shanghai, China) was used to monitor water distribution and migration. Detailedly, samples (2.00 ± 0.05 g) were placed into an NMR glass tube and removed into a 25 mm diameter nuclear magnetic coil, operated at 32 °C. The Carre-Purcell-Meiboom-Gill (CPMG) pulse sequence was adopted to test transverse relaxation time (T2) and corresponding peak areas (A2). The parameters were performed as follows: TW = 4500 ms, TE = 0.5 ms, NECH = 12,000, NS = 8, and total iterations number = 100,000.

2.4.2. Magnetic resonance imaging (MRI) analysis

The proton density images of salted radishes were obtained using a sequence of SPIN ECHO (SE) in a New Mai NMR imaging system (V1.23.03D), the detailed parameters are as follows: field of view = 100 mm × 100 mm, slice width = 3.0 mm, slice gap = 2.0 mm, average = 4, read size = 256, phase size = 192, TR (time repetition) = 500 ms, TE (time echo) = 20 ms. The final images were obtained by using the filter and unified map functions in the image processing software (version 1.0, New Mai Electric Co., Ltd., Shanghai, China).

2.5. Cell wall polysaccharides content determination

The micromethod assay was used to determine the content of total pectin, cellulose, hemicellulose, soluble pectin, chelator-soluble pectin, and alkali-soluble pectin, and 0.05 g sample was taken. All procedures were carried out according to the instructions of their respective content detection kits. To be specific, total pectin, WSP, CSP, and NSP were extracted using alkaline solution, water, chelating agent, and sodium carbonate, respectively. These pectins can be degraded into galacturonic acid under acidic conditions. The sulfuric acid-carbazole colorimetric method was then used to determine the pectin content (expressed as galacturonic acid content). The principle of this method is that galacturonic acid can undergo a condensation reaction with carbazole in a strong acid solution, forming a purple complex, with a maximum absorption peak at 530 nm. Cellulose can be thermally decomposed into β-glucose under acidic conditions. β-glucose, under the action of strong acid, can undergo dehydration to form β-furfural compounds. This compound can then undergo dehydration condensation with anthrone to produce furfural derivatives. Subsequently, the cellulose content can be quantified based on the intensity of color. Hemicellulose is converted into reducing sugars after acid treatment, forming a reddish-brown substance with 3,5-dinitrosalicylic acid (DNS), exhibiting a characteristic absorption peak at 540 nm, then the absorbance value reflects the hemicellulose content. All content units were expressed in mg/g dry weight (DW).

2.6. Cell wall polysaccharides-related enzyme activities determination

The double-antibody one-step sandwich enzyme-linked immunosorbent assay (ELISA) was employed to determine the activities of pectin methylesterase (PME), polygalacturonase (PG), cellulase, and hemicellulase, and 0.05 g sample was taken. All procedures were performed according to the instructions of the respective kit. The method of ELISA achieves high-sensitivity detection of the target molecule by simultaneously employing two specific antibodies on solid-phase support, with the addition of enzyme markers and the subsequent reaction with a substrate generating measurable changes in absorbance. Activity units were expressed in U/g.

2.7. SEM observations

Each sample tissue was cut into small pieces (approximately 0.4 cm × 0.2 cm × 0.1 cm), and fixed with 4% glutaraldehyde for 24 h. Thereafter, the samples were washed for 3 h with phosphate buffer solution (pH 7.2), 10 min each time. Then, samples were dehydrated with 30%, 50%, 60%, 70%, 80%, 90%, 95%, and 100% alcoholic solution, 15 min per gradient. After that, a critical point dryer (Leica CPD 030, USA) with CO_2 was used for sample drying. Before testing, stick the dried samples to the sample stage and make group records. The samples were sprayed with an ion sputtering instrument (HITACHI MC1000, Japan) and observed with a cold field-emission scanning electron microscope (HITACHI Regulus 8200, Japan).

2.8. Statistical analysis

The experiments were repeated three times in each group independently. Graphs were created using OriginPro 2019 (OriginLab Corp., Northampton, MA, USA). Analysis of variance (ANOVA) and Duncan's test was performed using SPSS Statistics 24.0 (IBM, Chicago, IL, USA) to determine the significance level ($p < 0.05$). All acquired data values were expressed as mean ± standard deviation (SD).

3. Results and discussion

3.1. Texture analysis

The hardness and brittleness changes of salted radish during the long-term dry-salting process are illustrated in Fig. 1A and B, the initial hardness and crispiness of fresh radish samples were 46.96 N and 6.35 mm, respectively. The longer the salting time, the hardness and crispness decreased ($P<0.05$), the greatest decline was observed in the later period (day 45 to 60) of salting, and the decline rates of the two indicators on the 60th day were approximately 66.33% and 54.53%, respectively, compared with that of fresh samples. This regular change differed from the trends in the salting processes of bamboo shoots, where texture initially increased and then decreased (Zhang, Zheng, Zhong, Chen, & Kan, 2016). In the salting stage, the ongoing decrease in texture parameters was associated with an increase in intercellular space, thinning of cell walls, and changes in the content of the primary components of pectin in a previous report (Ye et al., 2022). In the existing research results, the salting period (15 days as one salting stage) showed a significant negative correlation with hardness and crispiness indicators ($p<0.05$).

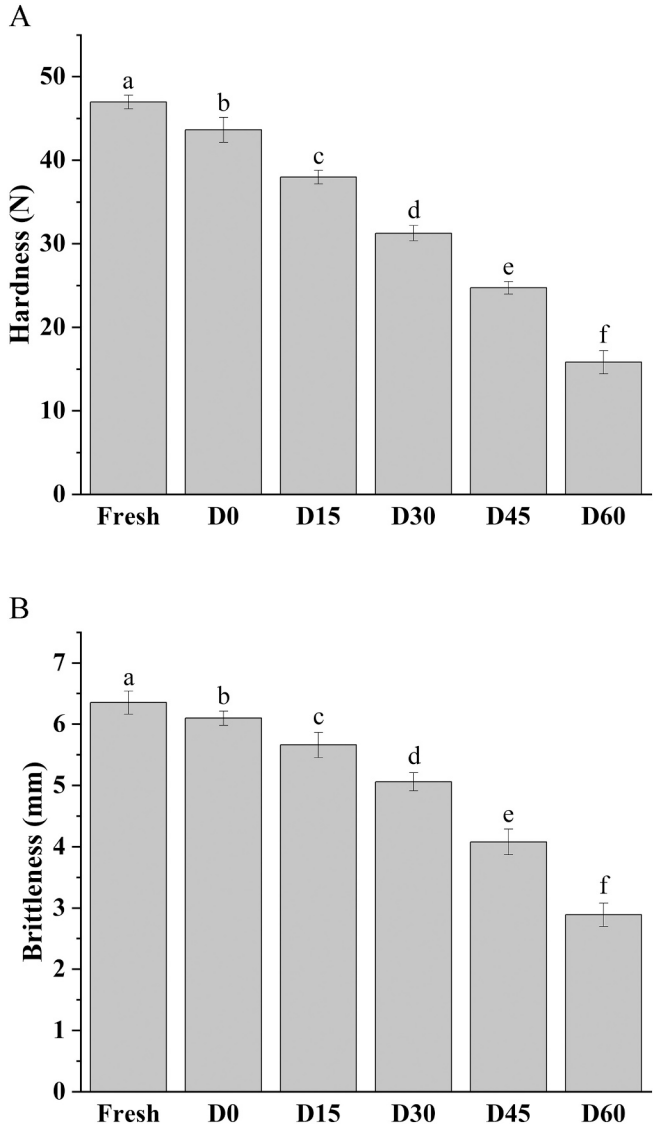

Fig. 1. Hardness (A) and brittleness (B) of dry-salting radish during the 60-day salting period. Different lowercase letters represent significantly different at a level of $p < 0.05$.

3.2. Water distribution

3.2.1. Transverse relaxation time analysis

The transverse relaxation time was frequently employed to elucidate the distribution and mobility of intracellular water (Shi et al., 2022). As depicted in Fig. 2A, three distinct hydrogen proton peaks emerged within the relaxation time range of 0.01–10,000 ms. These hydrogen proton peaks, are denoted as bound water (T21), immobilized water (T22), and free water (T23) according to the moving properties of water molecules (Zhang, Yu, Fan, & Sun, 2021). In line with the pattern observed in most fruits and vegetables, the relative content of free water was highest in radish samples, followed by immobilized water and bound water (Chao, Li, & Fan, 2023; Yao et al., 2021). Additionally, it can be observed that the transverse relaxation time of the fresh radish sample was the longest, with the highest peak amplitude. In the early stage of salting (day 0), the peak amplitude of free water decreased and the transverse relaxation time shifted to the left. This phenomenon is likely attributed to the loss of free water caused by osmotic pressure resulting from salting. Similar findings were also observed in the kohlrabi samples by Yang et al. (2023). Particularly, the peak amplitude of free water was significantly reduced at day 15. This could be attributed to the fact that sample tissues that have not adapted to the salting environment in the early stage were more susceptible to damage during the salting process, while the cells that had adapted to the salted environment showed a stronger external resistance (Mothibe, Zhang, Mujumdar, Wang, & Cheng, 2014). Therefore, although there was a decline in the peak amplitude of free water at day 60, it was not pronounced. Furthermore, with the prolonged salting period (day 45 to 60), the transverse relaxation time of free water exhibited a rightward shift, indicating increased water freedom, enhanced mobility, and decreased binding forces between water and cells (Cheng et al., 2017). A plausible explanation for this phenomenon is that the extended salting time led to damage in the cell wall structure (thinning of the cell wall, wrinkling instead of smoothness, and loosening instead of turgor), which prompted an enhancement in the flow dynamics of hydrogen protons, resulting in a weakening of the binding forces between water and radish tissues.

A21, A22, and A23 represent the relative content of different water components (Chen et al., 2020). It can be observed from Fig. 2B-D that A22 and A23 constituted the major portion of the samples with a proportion exceeding 98%, and dry-salting led to a regular increase in the relative contents of A21 and A22, while the relative proportion of A23 was reduced to a certain extent, which meant that the loss of the relative content of free water during the salting period was irreversible. This conclusion is largely consistent with the findings of Jiang et al. (2021), who stated that the microstructural damage to cell walls significantly caused tissue weight loss, and this indicator primarily manifested as the loss of free water, followed by immobile water and bound water. Transverse relaxation time and relative water content are not sufficient to visually visualize water distribution and transfer, therefore, magnetic resonance imaging (MRI) analysis is necessary.

3.2.2. MRI analysis

Based on the principle of LF-NMR, MRI can directly observe the spatial distribution of water molecules in samples. The hydrogen proton density of radish tissues at different salting stages is depicted in Fig. 2E.

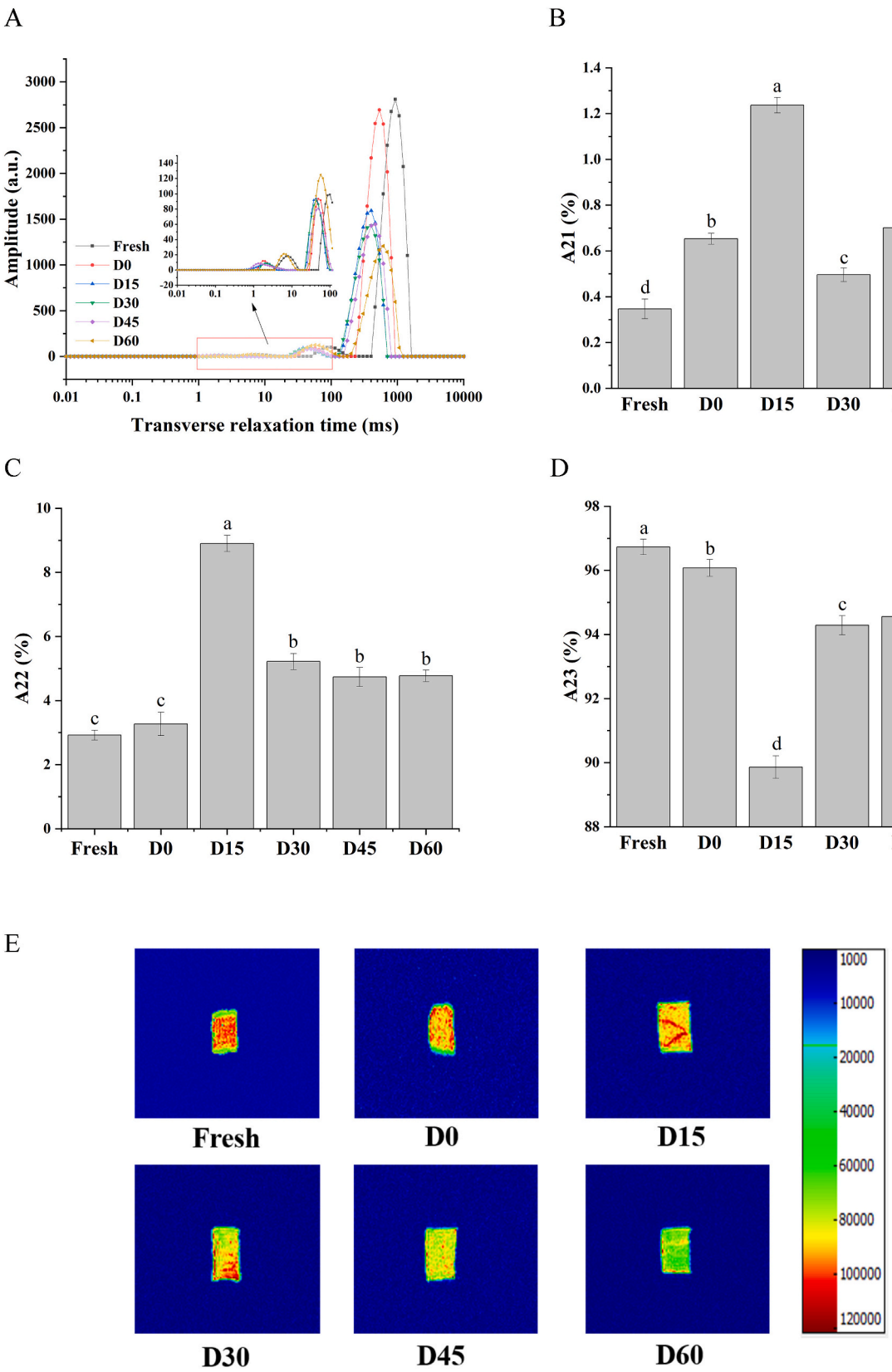

Fig. 2. Carr-Purcell-Meiboom-Gill (CPMG) proton distribution (A), T2 relative area (B, C, and D), and proton density maps (E) of dry-salting radish during the 60-day salting period.

Using the pseudo-color scale as a reference, the transition of hydrogen proton density from low to high is defined by shifting from blue to red (Gu et al., 2022). As illustrated in the images, the hydrogen proton density in fresh salted radish was uniformly distributed and concentrated throughout the entire tissue of the sample (excluding the edges). After salting, both the density and uniformity of hydrogen protons were visibly reduced. After the 60-day salting period, the water distribution of the sample was reduced, and was even scattered only in the edge regions of the tissue, which represented the transfer and loss of water from the center to the outside. This phenomenon is consistent with the findings of the study conducted by Yang et al. (2023), who convinced that salting-out action promoted the reduction of water components after cell wall damage and facilitated tissue dehydration.

4. Cell wall polysaccharides content and related enzyme activities

4.1. Cellulose, hemicellulose content, and related enzyme activities

Cellulose, as a structural polysaccharide capable of forming microfibers in the cell wall, plays a beneficial role in supporting cell structure and maintaining cell integrity and rigidity. Its functional properties contribute to the texture maintenance of plant tissues (Wang, Elliott, & Williamson, 2008). Hemicellulose is a heterogeneous polysaccharide primarily composed of xyloglucan (XyG) and xylan (Xyl). Physical cross-linking through hydrogen bonds occurs between cellulose microfibers and hemicellulose polymers, forming a complex network structure, with pectin polysaccharides embedded within this network (Miyamoto et al., 2022). When either was degraded, the hydrogen bonds between the two were disrupted, leading to the breakdown of the intricate network structure (Zhang et al., 2022). Therefore, pectin is closely related to cellulose and hemicellulose, and this relationship has been valued by researchers. As observed in Fig. 3A-B, the cellulose and hemicellulose contents in fresh radish samples were highest, which were 43.17 ± 1.04 mg/g DW and 30.94 ± 1.84 mg/g DW, respectively. Subsequently, with the extension of the salting period, there was a significant downward trend in both indexes. At the end of the salting period, they dropped to 28.26 ± 0.54 mg/g DW (a decrease rate of 34.54%) and 22.47 ± 0.49 mg/g DW (a decrease rate of 27.38%), respectively. The overall results meant that the content of cellulose and hemicellulose were prone to degradation in the salting environment, a process likely triggered by exogenous enzymes released by microbes in the environment and the corresponding release of endogenous enzymes (cellulases and hemicellulases) within the tissues (Mcfeeters, 2010). In this study, the activities of cellulase and hemicellulase were the lowest in the fresh sample, and then gradually increased. On the 60th day, they increased to 1.82 and 1.42 times their respective original content (Fig. 3C-D). In conclusion, the enzyme activity results were consistent

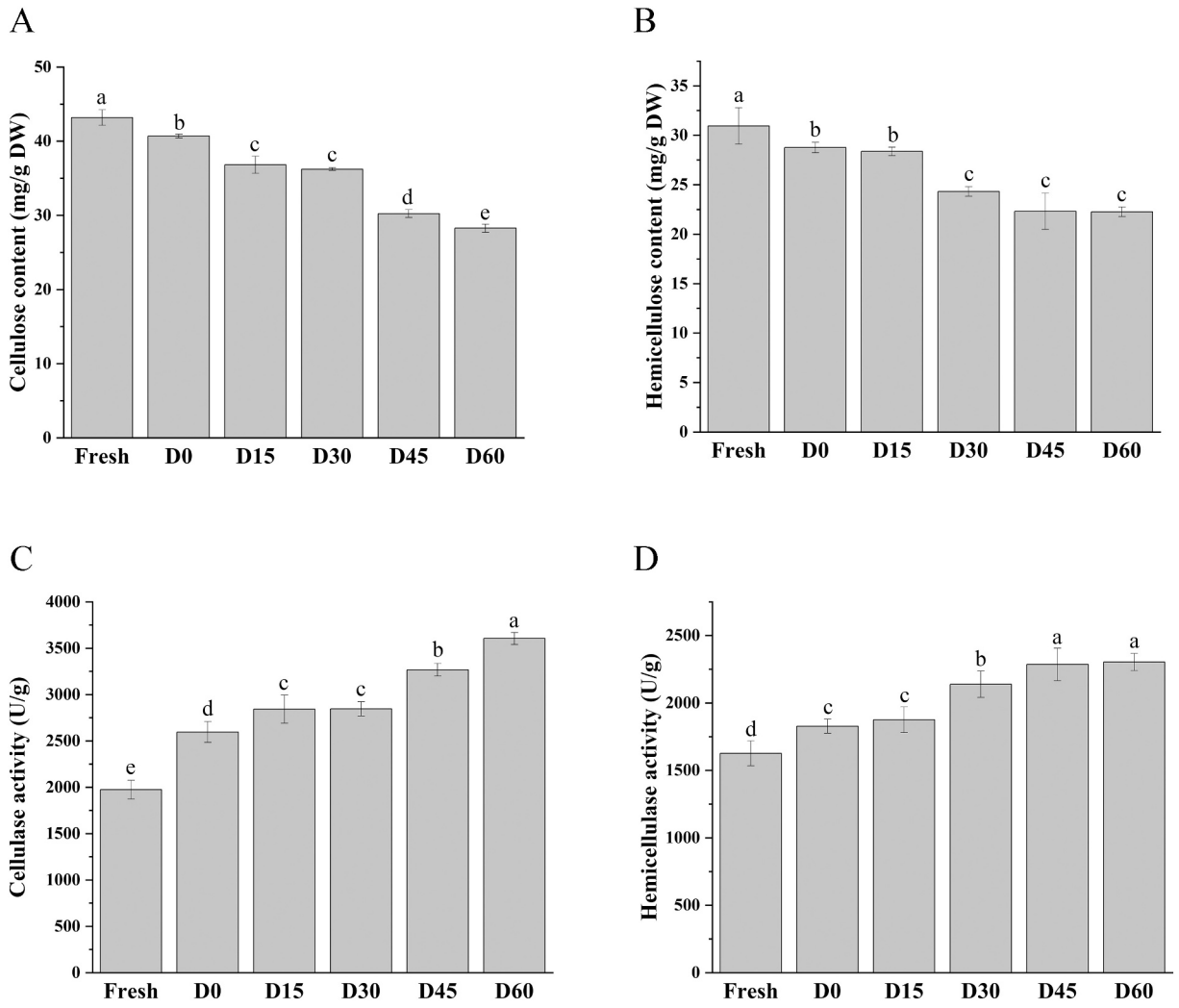

Fig. 3. The content of cellulose (A) and hemicellulose (B), and the activities of cellulase (C) and hemicellulase (D) of dry-salting radish during the 60-day salting period.

with the enzyme content outcomes, collectively revealing a pronounced regularity in the degradation of cellulose and hemicellulose in salted radishes during an extended dry-salting process.

4.2. Pectin content and related enzyme activities

As a complex biopolymer, pectin consists of the primary cell wall and middle lamella, contributing to enhanced cell adhesion and mechanical strength (Lv et al., 2021). Total pectin contains three forms (WSP, ASP, and CSP), and determining pectin content aids in advancing the exploration of the pectin impact mechanism on the texture of salted radish (Liu, Liang, Jiang, & Chen, 2019). From Fig. 4A, total pectin content showed a pronounced downward trend ($p<0.05$), especially in the later stages of salting (days 45 to 60). This result is consistent with the findings of Wongkaew et al. (2021), who proposed endogenous pectinases in fruits and vegetables degraded total pectin into soluble oligosaccharides

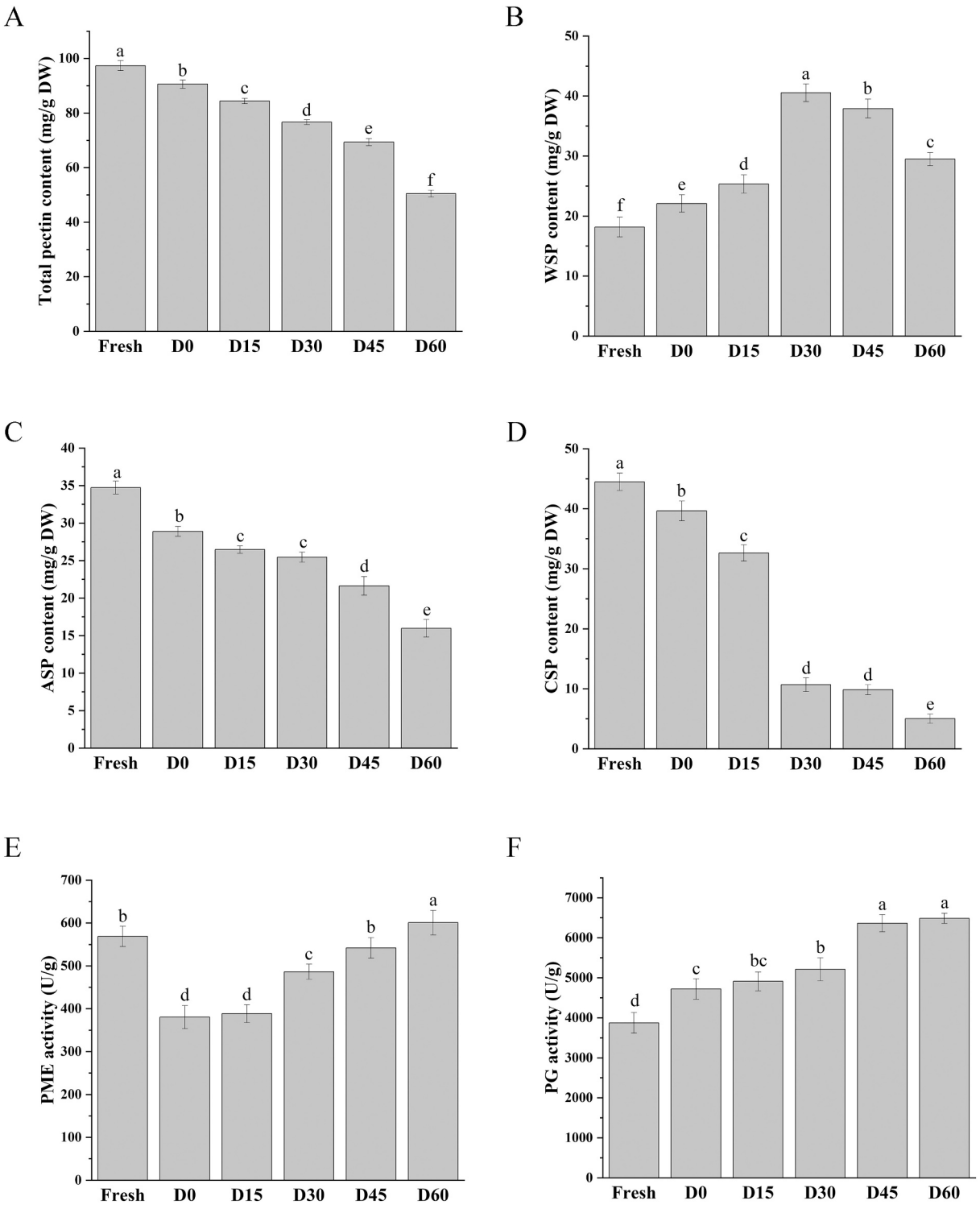

Fig. 4. The content of total pectin (A), water-soluble pectin (B), alkali-soluble pectin (C), and chelator-soluble pectin (D), and the activities of pectin methylesterase (E) and polygalacturonase (F) of dry-salting radish during the 60-day salting period. DW, dry weight.

or free monosaccharides, leading to continuous reduction of total pectin content.

The CSP exhibited the highest content in fresh radish tissues, followed by ASP and WSP, with content of 44.49 ± 1.46 mg/g DW, 34.73 ± 0.86 mg/g DW, and 18.16 ± 0.66 mg/g DW, respectively (Fig. 4B-D). This compositional ratio is similar with the findings of Deng, Wu, and Li (2005) in grapes. During the salting process, the WSP content exhibited an initial increase (day 0 to day 30) followed by a subsequent decline (day 30 to day 60), while ASP and CSP showed a consistent decreasing trend, which was most pronounced at the late stage of salting. ASP typically binds to cell wall polysaccharides through covalent bonds, forming a polysaccharide network that plays a key role in the stability of the primary cell wall. The significant decrease in ASP during the dry-salting period weakened the strength of the cell wall, leading to a thinning of the cell wall thickness and promoting a looser connection among cells (Liu et al., 2017). CSP primarily interacts with calcium ions in the cell wall through ionic bonds, influencing cell adhesion. The reduction in CSP content disrupted the connections among cells in salted radish tissues, resulting in loose intercellular spaces that were adverse for maintaining hardness (Zdunek, Kozioł, Pieczywek, & Cybulska, 2014). Studies have indicated that the breakage of ionic bonds in polysaccharides converts CSP into WSP (Sun et al., 2022). Additionally, the demethylation reaction of pectin under the action of PME led to an increase in hydroxyl groups, enhancing the hydrophilicity of pectin and making CSP more prone to conversion into WSP. Therefore, the overall upward trend in WSP content during the dry-salting period could visually reflect the degree of degradation of pectin substances (Imaizumi et al., 2017). Noteworthily, the WSP content exhibited a relative decrease on day 45 and day 60. We speculate that this was mainly due to the severe degradation and disruption of the cell wall structure, leading to the rapid loss of the cytoplasm, in which WSP is located, even though the CSP may still be undergoing the conversion to WSP during this process (Einhorn-Stoll, Kastner, & Drusch, 2014). The changing trends of these three pectin fractions were similar to the trends observed in various fruits and vegetables during the softening process, and these changes were commonly explained as hydrolysis phenomena resulting from the collaborative action of PME and PG (Paniagua et al., 2014; Yuliarti et al., 2015).

Pectin metabolism can greatly affect cell wall properties (Zhang et al., 2022). Pectin methylation is one of the manifestations of pectin metabolism and can affect the biomechanical properties of cell walls (Wormit & Usadel, 2018). PME can promote the demethylation of pectin, and the low-esterification pectin can further combine with calcium ions to enhance the rigidity of the cell wall, thus increasing the texture of fruits and vegetables (Yan, Han, Fu, Jiao, & Wang, 2021). As shown in Fig. 4E, compared to the fresh samples, the activity of PME exhibited a decreasing trend in the early stages of salting (day 0–15). Given the enzymatic nature of PME as a protein, we speculate that the decline in PME activity is likely due to the adverse effects of salt on its active sites, causing a substantial loss of its catalytic properties. This speculation is consistent with the viewpoint of Ge et al. (2021). Subsequently, PME activity showed a significant upward trend, with the most pronounced increase in the later stages of salting (days 45–60). Research has shown that PME could bind to the cell wall through electrostatic interactions, and the destruction of the cell wall caused by salting could release more PME, increasing its overall activity (Wormit & Usadel, 2018).

As a pectin-degrading enzyme, PG can participate in the decomposition of the galacturonic acid backbone, leading to a decrease in cell rigidity and adverse effects on tissue texture (Yi et al., 2016). As illustrated in Fig. 4F, the PG activity showed an overall regular increase trend, with the most significant elevation observed in the later stages of salting (day 45–60), which was 1.67 times that of the initial stage. This phenomenon was distinct from that of pectin methylesterase (PME). Taking the functional properties of PG into consideration, this finding can be explained by the following viewpoints: PG can effectively recognize the deesterified neutral HG pectin chain and promote the decomposition of cell wall pectin (Ayour et al., 2021). During the early stages of salting, PME's low activity prevented it from participating in the demethylation of pectin, resulting in an insufficient supply of catalytic substrates for PG, causing it to lose enzymatic catalytic performance. Subsequently, the severe loss of the cell wall led to the release of PG, which worked with PME to promote the hydrolysis of cell wall pectin polymers, ultimately causing a decline in the texture and crispness of salted radish (Lu et al., 2021).

5. SEM observations

The SEM, with its wide observation range and capability to effectively depict the three-dimensional morphology of samples, was employed to elucidate the relationship between the texture changes of radishes during the dry-salting process and the microstructure of cell walls and intracellular substances. From Fig. 5, it can be observed that the fresh, unsalted radish tissues exhibited a regular elliptical-shaped parenchymatous tissue, and the middle lamella also had a well-defined feature. However, as the salting period advanced, the cell walls underwent turgor loss, resulting in a gradual shrinkage and collapse of the cell profile. Moreover, the middle lamella underwent thinning, progressively losing its adhesion properties, thereby leading to enlarged intercellular space and noticeable separation. After the salting period, the cell walls of the radish samples had undergone complete wrinkling, with severe shape distortion, and the middle lamella had entirely lost its adhesive properties. These visual outcomes vividly illustrated the rupture of the microcellular structure after prolonged salting, and this phenomenon is similar to the trend of microscopic structural changes observed during the salting period of cucumbers and carrots (Llorca et al., 2001; Yoo, Hwang, Eog, & Moon, 2006).

6. Speculated mechanism of changes in textural properties

We hypothesized that the textural changes in salted radish underwent the following processes: in the long-term dry-salting process, the activities of cellulase and hemicellulase significantly enhanced, which directly stimulated the degradation of cellulose and hemicellulose, leading to the rupture of their structures. Additionally, the substantial release of PME and PG, along with their interaction, directly contributed to the overall loss of total pectin. This phenomenon was accompanied by a simultaneous decrease in ASP and CSP content, while the WSP content increased. The comprehensive depolymerization and degradation of cell wall polysaccharides accelerated the shrinkage and wrinkles of the cell wall, and at the same time enlarged the intercellular spaces. The above results were mutually verified with the findings of low-field NMR (water was lost and transferred from the internal to the surface of the tissues). Eventually, a notable decline in the hardness and crispness of salted radish was observed with the prolonged salting period (Fig. 6).

7. Conclusion

The changes in textural properties and the factors affecting the texture of radish during long-term dry-salting at 4 °C for 60 days were studied. Prolonged salting resulted in a significant decrease in the hardness and crispiness of salted radishes, which was associated with overall increases in content of water-soluble pectin (WSP) and activities of cellulase and polygalacturonase (PG), and gradual decreases in total pectin, ASP, CSP, cellulose, and hemicellulose content. SEM observations revealed that prolonged salting time caused a reduction in cell turgor, increased wrinkling of cell walls, and a gradual loss of adhesion capability in the middle lamella. Moreover, dry-salting accelerated samples' water loss and transfer. The research findings can provide targeted guidance for maintaining the texture of radishes in the step of dry-salting processing.

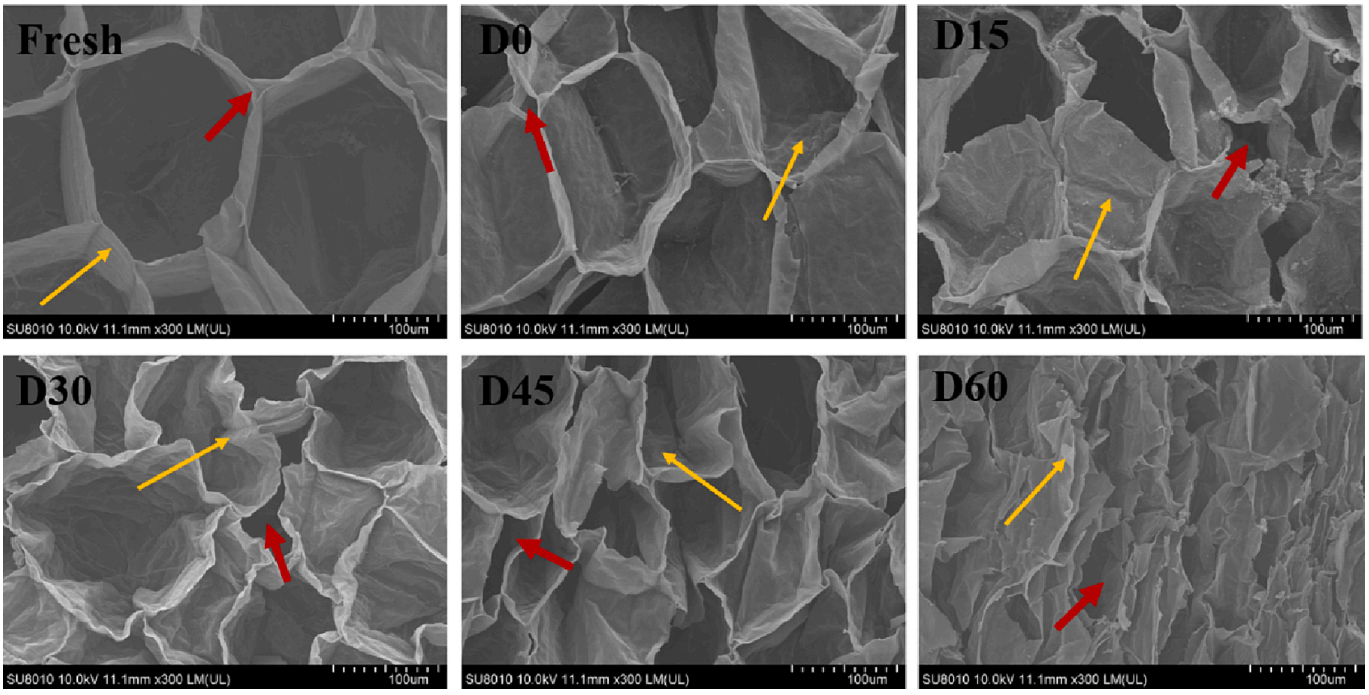

Fig. 5. SEM images (magnification 300 times) of dry-salting radish during the 60-day salting period. Short arrows (red) indicate intracellular space and long arrows (yellow) indicate cell wall shrinkage. (For interpretation of the references to color in this figure legend, the reader is referred to the web version of this article.)

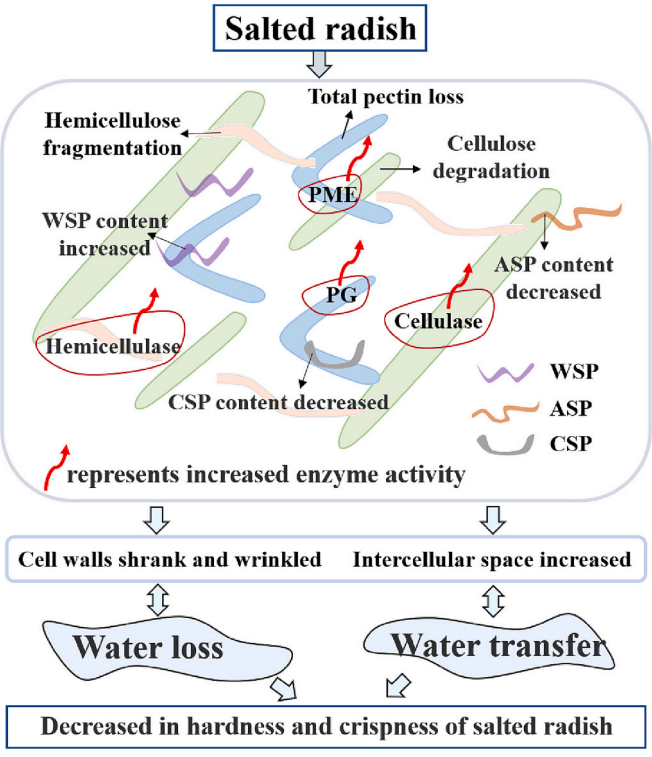

Fig. 6. Hypothetical mechanism of dry-salting radish texture changes during the 60-day salting period.

CRediT authorship contribution statement

Qianqian Jiang: Writing – original draft, Methodology, Investigation. **Shuang Zhao:** Formal analysis, Data curation. **Wenting Zhao:** Formal analysis, Data curation. **Peiyou Qin:** Formal analysis, Data curation. **Junjuan Wang:** Formal analysis, Data curation. **Yuanyuan Zhao:** Formal analysis, Data curation. **Zhiwen Ge:** Formal analysis, Data curation. **Xiaoyan Zhao:** Writing – review & editing, Funding acquisition, Conceptualization. **Dan Wang:** Writing – review & editing, Funding acquisition, Conceptualization.

Declaration of competing interest

The authors declare that they have no known competing financial interests or personal relationships that could have appeared to influence the work reported in this paper.

Data availability

Data will be made available on request.

Acknowledgments

This work was supported by National Key Research and Development Program of China (2022YFD1602402), the Scientific and Technological Innovation Ability Foundation of Beijing Academy of Agricultural and Forestry Sciences (KJCX20230211), Collaborative Innovation Center of the Beijing Academy of Agricultural and Forestry Sciences (KJCX20240402), Major Scientific and Technological Achievements Cultivation Project of Beijing Academy of Agriculture and Forestry Sciences, and Agriculture Research System of China of MOF and MARA (CARS-23).

References

Ayour, J., Le Bourvellec, C., Gouble, B., Audergon, J. M., Benichou, M., & Renard, C. (2021). Changes in cell wall neutral sugar composition related to pectinolytic enzyme activities and intra-flesh textural property during ripening of ten apricot clones. *Food Chemistry, 339*, Article 128096. https://doi.org/10.1016/j.foodchem.2020.128096

Chao, E., Li, J., & Fan, L. (2023). Influence of combined freeze-drying and far-infrared drying technologies on physicochemical properties of seed-used pumpkin. *Food Chemistry, 398*, Article 133849. https://doi.org/10.1016/j.foodchem.2022.133849

Chen, Y., Li, M., Dharmasiri, T. S. K., Song, X., Liu, F., & Wang, X. (2020). Novel ultrasonic-assisted vacuum drying technique for dehydrating garlic slices and

predicting the quality properties by low field nuclear magnetic resonance. *Food Chemistry, 306*, Article 125625. https://doi.org/10.1016/j.foodchem.2019.125625
Cheng, S., Tang, Y., Zhang, T., Song, Y., Wang, X., Wang, H., … Tan, M. (2017). Approach for monitoring the dynamic states of water in shrimp during drying process with LF-NMR and MRI. *Drying Technology, 36*(7), 841–848. https://doi.org/10.1080/07373937.2017.1357569
Deng, Y., Wu, Y., & Li, Y. (2005). Changes in firmness, cell wall composition and cell wall hydrolases of grapes stored in high oxygen atmospheres. *Food Research International, 38*(7), 769–776. https://doi.org/10.1016/j.foodres.2005.03.003
Einhorn-Stoll, U., Kastner, H., & Drusch, S. (2014). Thermally induced degradation of citrus pectins during storage – Alterations in molecular structure, colour and thermal analysis. *Food Hydrocolloids, 35*, 565–575. https://doi.org/10.1016/j.foodhyd.2013.07.020
Gamba, M., Asllanaj, E., Raguindin, P. F., Glisic, M., Franco, O. H., Minder, B., … Muka, T. (2021). Nutritional and phytochemical characterization of radish (*Raphanus sativus*): A systematic review. *Trends in Food Science & Technology, 113*, 205–218. https://doi.org/10.1016/j.tifs.2021.04.045
Ge, L., Lai, H., Huang, Y., Wang, Y., Li, Y., Zhu, S., … Zhao, N. (2021). Comparative evaluation of package types in alleviating textural softening and package-swelling of Paocai during storage: Insight into microbial invasion, cell wall pectinolysis and alteration in sugar and organic acid profiles. *Food Chemistry, 365*, Article 130489. https://doi.org/10.1016/j.foodchem.2021.130489
Gu, Y., Chen, Y., Yue, X., Xiong, P., Pan, D., Song, P., & Luo, B. (2022). LF-NMR/MRI determination of different 6-benzylaminopurine concentrations and their effects on soybean moisture. *Frontiers in Plant Science, 13*, Article 885804. https://doi.org/10.3389/fpls.2022.885804
Imaizumi, T., Szymańska-Chargot, M., Pieczywek, P. M., Chylińska, M., Kozioł, A., Ganczarenko, D., … Zdunek, A. (2017). Evaluation of pectin nanostructure by atomic force microscopy in blanched carrot. *LWT, 84*, 658–667. https://doi.org/10.1016/j.lwt.2017.06.038
Jiang, L., Luo, Z., Liu, H., Wang, F., Li, H., Gao, H., & Zhang, H. (2021). Preparation and characterization of chitosan films containing lychee (*Litchi chinensis* Sonn.) pericarp powder and their application as active food packaging. *Foods, 10*(11). https://doi.org/10.3390/foods10112834
Li, X., Wang, W., Wang, Y., Cui, W., Liu, L., & Xu, Z. (2018). Effects of exogenous pectin methylesterase on texture properties of low-salt pickled cucumber. *Journal of Food Science and Technology, 36*(06), 88–94. https://doi.org/10.3969/j.issn.2095-6002.2018.06.013
Liu, A., Li, X., Pu, B., Ao, X., Zhou, K., He, L., … Liu, S. (2017). Use of psychrotolerant lactic acid bacteria (*Lactobacillus* spp. and *Leuconostoc* spp.) isolated from Chinese traditional paocai for the quality improvement of Paocai products. *Journal of Agricultural and Food Chemistry, 65*(12), 2580–2587. https://doi.org/10.1021/acs.jafc.7b00050
Liu, H., Chen, F., Lai, S., Tao, J., Yang, H., & Jiao, Z. (2017). Effects of calcium treatment and low temperature storage on cell wall polysaccharide nanostructures and quality of postharvest apricot (*Prunus armeniaca*). *Food Chemistry, 225*, 87–97. https://doi.org/10.1016/j.foodchem.2017.01.008
Liu, J., Liang, L., Jiang, Y., & Chen, J. (2019). Changes in metabolisms of antioxidant and cell wall in three pummelo cultivars during postharvest storage. *Biomolecules, 9*(8). https://doi.org/10.3390/biom9080319
Llorca, E., Puig, A., Hernando, I., Salvador, A., Fiszman, S. M., & Lluch, M. A. (2001). Effect of fermentation time on texture and microstructure of pickled carrots. *Journal of the Science of Food and Agriculture, 81*(15), 1553–1560. https://doi.org/10.1002/jsfa.975
Lu, R., Ma, Y., Wang, X., Zhao, X., Liang, H., & Wang, D. (2021). Study of texture properties of 'laba' garlic in different color states and their change mechanisms. *International Journal of Food Science & Technology, 56*(9), 4710–4721. https://doi.org/10.1111/ijfs.15222
Lv, J., Zheng, T., Song, Z., Pervaiz, T., Dong, T., Zhang, Y., … Fang, J. (2021). Strawberry proteome responses to controlled hot and cold stress partly mimic post-harvest storage temperature effects on fruit quality. *Frontiers in Nutrition, 8*, Article 812666. https://doi.org/10.3389/fnut.2021.812666
Mcfeeters, R. F. (2010). Cell wall monosaccharide changes during softening of brined cucumber mesocarp tissue. *Journal of Food Science, 57*(4), 937–940. https://doi.org/10.1111/j.1365-2621.1992.tb14328.x
Miyamoto, T., Tsuchiya, K., Toyooka, K., Goto, Y., Tateishi, A., & Numata, K. (2022). Relaxation of the plant cell wall barrier via zwitterionic liquid pretreatment for micelle-complex-mediated DNA delivery to specific plant organelles. *Angewandte Chemie (International Ed. in English), 61*(32), Article e202204234. https://doi.org/10.1002/anie.202204234
Mothibe, K. J., Zhang, M., Mujumdar, A. S., Wang, Y. C., & Cheng, X. (2014). Effects of ultrasound and microwave pretreatments of apple before spouted bed drying on rate of dehydration and physical properties. *Drying Technology, 32*(15), 1848–1856. https://doi.org/10.1080/07373937.2014.952381
Paniagua, C., Pose, S., Morris, V. J., Kirby, A. R., Quesada, M. A., & Mercado, J. A. (2014). Fruit softening and pectin disassembly: An overview of nanostructural pectin modifications assessed by atomic force microscopy. *Annals of Botany, 114*(6), 1375–1383. https://doi.org/10.1093/aob/mcu149
Shi, H., Ali Khan, I., Zhang, R., Zou, Y., Xu, W., & Wang, D. (2022). Evaluation of ultrasound-assisted (L)-histidine marination on beef M. Semitendinosus: Insight into meat quality and actomyosin properties. *Ultrasonics Sonochemistry*. , Article 105987. https://doi.org/10.1016/j.ultsonch.2022.105987
Sun, J., Chen, H., Xie, H., Li, M., Chen, Y., Hung, Y. C., & Lin, H. (2022). Acidic electrolyzed water treatment retards softening and retains cell wall polysaccharides in pulp of postharvest fresh longans and its possible mechanism. *Food Chemistry: X, 13*, Article 100265. https://doi.org/10.1016/j.fochx.2022.100265
Wang, J., Elliott, J. E., & Williamson, R. E. (2008). Features of the primary wall CESA complex in wild type and cellulose-deficient mutants of Arabidopsis thaliana. *Journal of Experimental Botany, 59*(10), 2627–2637. https://doi.org/10.1093/jxb/ern125
Wei, W., Hu, X., Yang, S., Wang, K., Zeng, C., Hou, Z., … Zhu, L. (2022). Denitrifying halophilic archaea derived from salt dominate the degradation of nitrite in salted radish during pickling. *Food Research International, 152*, Article 110906. https://doi.org/10.1016/j.foodres.2021.110906
Wongkaew, M., Tinpovong, B., Sringarm, K., Leksawasdi, N., Jantanasakulwong, K., Rachtanapun, P., … Sommano, S. R. (2021). Crude pectic oligosaccharide recovery from thai chok anan mango peel using pectinolytic enzyme hydrolysis. *Foods, 10*(3). https://doi.org/10.3390/foods10030627
Wormit, A., & Usadel, B. (2018). The multifaceted role of pectin methylesterase inhibitors (PMEIs). *International Journal of Molecular Sciences, 19*(10). https://doi.org/10.3390/ijms19102878
Yan, R., Han, C., Fu, M., Jiao, W., & Wang, W. (2021). Inhibitory effects of $CaCl_2$ and pectin methylesterase on fruit softening of raspberry during cold storage. *Horticulturae, 8*(1). https://doi.org/10.3390/horticulturae8010001
Yang, Z., Fan, H., Li, R., Li, B., Fan, J., Ge, J., … Liu, F. (2023). Potential role of cell wall pectin polysaccharides, water state, and cellular structure on twice "increase-decrease" texture changes during kohlrabi pickling process. *Food Research International, 173*, Article 113308. https://doi.org/10.1016/j.foodres.2023.113308
Yao, Y., Sun, Y., Cui, B., Fu, H., Chen, X., & Wang, Y. (2021). Radio frequency energy inactivates peroxidase in stem lettuce at different heating rates and associate changes in physiochemical properties and cell morphology. *Food Chemistry, 342*, Article 128360. https://doi.org/10.1016/j.foodchem.2020.128360
Ye, Z., Shang, Z., Li, M., Zhang, X., Ren, H., Hu, X., & Yi, J. (2022). Effect of ripening and variety on the physiochemical quality and flavor of fermented Chinese chili pepper (Paojiao). *Food Chemistry, 368*, Article 130797. https://doi.org/10.1016/j.foodchem.2021.130797
Ye, Z., Shang, Z., Zhang, S., Li, M., Zhang, X., Ren, H., … Yi, J. (2022). Dynamic analysis of flavor properties and microbial communities in Chinese pickled chili pepper (*Capsicum frutescens* L.): A typical industrial-scale natural fermentation process. *Food Research International, 153*. https://doi.org/10.1016/j.foodres.2022.110952
Yi, J., Kebede, B. T., Grauwet, T., Van Loey, A., Hu, X., & Hendrickx, M. (2016). A multivariate approach into physicochemical, biochemical and aromatic quality changes of purée based on Hayward kiwifruit during the final phase of ripening. *Postharvest Biology and Technology, 117*, 206–216. https://doi.org/10.1016/j.postharvbio.2016.03.007
Yoo, K. M., Hwang, I. K., Eog, G., & Moon, B. (2006). Effects of salts and preheating temperature of brine on the texture of pickled cucumbers. *Journal of Food Science, 71*(2). https://doi.org/10.1111/j.1365-2621.2006.tb08889.x
Yuliarti, O., Matia-Merino, L., Goh, K. K. T., Mawson, J., Williams, M. A. K., & Brennan, C. (2015). Characterization of gold kiwifruit pectin from fruit of different maturities and extraction methods. *Food Chemistry, 166*, 479–485. https://doi.org/10.1016/j.foodchem.2014.06.055
Zdunek, A., Kozioł, A., Pieczywek, P. M., & Cybulska, J. (2014). Evaluation of the nanostructure of pectin, hemicellulose and cellulose in the cell walls of pears of different texture and firmness. *Food and Bioprocess Technology, 7*(12), 3525–3535. https://doi.org/10.1007/s11947-014-1365-z
Zhang, F., Zheng, J., Zhong, J., Chen, G., & Kan, J. (2016). Kinetics of texture change of bamboo shoots during pickling process. *Journal of Food Process Engineering, 40*(2). https://doi.org/10.1111/jfpe.12369
Zhang, J., Yu, P., Fan, L., & Sun, Y. (2021). Effects of ultrasound treatment on the starch properties and oil absorption of potato chips. *Ultrasonics Sonochemistry, 70*, Article 105347. https://doi.org/10.1016/j.ultsonch.2020.105347
Zhang, P., Zu, W., Xue, Y., Li, C., Jia, X., & Li, J. (2022). Effects of micro-environment gas regulation on fruit softening of blueberry during shelf life after controlled freezing-point storage. *Journal of Food Science and Technology, 40*(3), 157–166. https://doi.org/10.16429/j.1009-7848.2022.05.027
Zhang, Z., Ge, M., Guo, Q., Jiang, Y., Jia, W., Gao, L., & Hu, J. (2022). Ultrahigh-throughput screening of high-beta-xylosidase-producing penicillium piceum and investigation of the novel beta-xylosidase characteristics. *Journal of Fungi (Basel), 8*(4). https://doi.org/10.3390/jof8040325